JACS
JOURNAL OF THE AMERICAN CHEMICAL SOCIETY

ARTICLE

pubs.acs.org/JACS

Using Si and Ge Nanostructures as Substrates for Surface-Enhanced Raman Scattering Based on Photoinduced Charge Transfer Mechanism

Xiaotian Wang,[†,‡] Wensheng Shi,[*,†] Guangwei She,[†] and Lixuan Mu[†]

[†]Key Laboratory of Photochemical Conversion and Optoelectronic Materials, Technical Institute of Physics and Chemistry, Chinese Academy of Sciences, Beijing 100190, China

[‡]Graduate School of Chinese Academy of Sciences, Beijing 100039, China

Supporting Information

ABSTRACT: The possibility of utilizing the Si and Ge nanostructures to promote surface-enhanced Raman scattering (SERS) is discussed. The vibronic coupling of the conduction band and valence band states of Si or Ge with the excited and ground states of the target molecule during the charge transfer (CT) process could enhance the molecular polarizability tensor. Using H-terminated silicon nanowire (H-SiNW) and germanium nanotube (H-GeNT) arrays as substrates, significant Raman enhancement of the standard probes, Rodamine 6G (R6G), dye $(Bu_4N)_2[Ru(dcbpyH)_2(NCS)_2]$ (N719), and 4-aminothiophenol (PATP), are demonstrated. The abundant hydrogen atoms terminated on the surface of SiNW and GeNT arrays play a critical role in promoting efficient CT and enable the SERS effect.

INTRODUCTION

The extremely high sensitivity and selectivity of surface-enhanced Raman scattering (SERS) enable potential applications in biochemical analysis.[1] However, SERS has not been developed as a technology as a chemosensor as initially predicted.[2] The major obstacle is that only several noble metals and transition metals exhibit significant SERS,[3−6] and these have poor biocompatibility. Recently, semiconductor materials have been sought as SERS active substrates. For example, the SERS effect from pyridine molecules adsorbed on InAs/GaAs quantum dots has been reported.[7] Moreover, the SERS effects from analytes on the surfaces of oxides such as ZnO,[8] TiO_2,[9] and α-Fe_2O_3[10] have also been reported. Also, from biocompatibility and stability perspectives, silicon (Si) and germanium (Ge) have been widely used in biochips, microprobes in biology and medicine.[11,12] In addition, the Si- and Ge-based devices would be compatible with current integration technology. In summary, SERS from the Si or Ge substrates would be noteworthy to widen the application of the Si and Ge in biochemical detection. Moreover, combining the observation of the SERS activity of graphene,[13] the investigation of SERS with Si and Ge substrates would also assist in the understanding of the mechanism of SERS of group IV materials. Normally, an electromagnetic mechanism (EM) and a chemical mechanism (CM) are widely accepted as the mechanisms for SERS.[14] The EM is based on the surface plasmon resonance excited by the incident light on the rough surfaces of a metal.[15−17] By contrast, CM is based on a charge transfer (CT) between target molecules and the substrate, which can enormously magnify the molecular polarizability tensor and result in SERS.[18−22] In principle, Si and Ge cannot have plasmon contributions in the visible region.[21] However, we explore the possibilities of SERS from Si or Ge substrates based on the CM mechanism.

In this work, we report a model of SERS in a semiconductor−molecule system based on the Herzberg−Teller theory.[20−22] It is found that tightly adsorbed molecules with matched highest occupied molecular orbital (HOMO) levels and lowest unoccupied molecular orbital (LUMO) levels to the semiconductor substrate could theoretically produce a thermodynamically allowed CT process. Such a CT process could enhance the molecular polarizability tensor through the vibronic coupling of the conduction band (CB) and valence band (VB) states of the semiconductor with the excited and ground states of the probe molecule, resulting in Raman scattering enhancement from the semiconductor substrate (the details are provided in the Supporting Information). Therefore, realization of an efficient CT process between the probe molecule and the Si or Ge substrate is key to realizing SERS. We explored possible approaches to increase the efficiency of CT processes between probe molecules and nanostructured Si or Ge substrates. On the basis of the alignment of the CB and VB of the Si or Ge substrates with the HOMO and LUMO of the probe molecules in the thermodynamically allowed CT process, and the enhancement effect of H-terminated Si nanowires (H-SiNWs) and Ge nanotube (H-GeNT) arrays on the CT efficiency,[23] SERS was exhibited by the standard probe Rodamine 6G (R6G), dye $(Bu_4N)_2[Ru(dcbpyH)_2(NCS)_2]$ (N719), and 4-aminothiophenol (PATP) using H-SiNW and H-GeNT arrays substrates.

Received: June 22, 2011
Published: September 22, 2011

dx.doi.org/10.1021/ja2057874 | J. Am. Chem. Soc. 2011, 133, 16518–16523

RESULTS AND DISCUSSION

SiNW arrays having CB and VB of −4.0 eV and −5.1 eV, respectively,[24] were fabricated by a modified Peng's method.[25] Briefly, a cleaned n-type silicon wafer with [100] orientation was immersed into a 5% hydrofluoric acid (HF) solution to form Si−H bonds on the surface of the wafer. Subsequently, the wafer was soaked in a 5 mM silver nitrate solution to deposit Ag particles on its surface. Ag particles act as a catalyst in the subsequent etching process. Wafers with Ag particles were soaked in an etching solution (4.8 M HF and 0.2 M H_2O_2) at 45 °C for 15 min to produce the SiNW arrays. Finally, the residual silver particles on the SiNW arrays were completely removed by soaking in an aqua regia solution;[26] this was further corroborated by angle-resolved XPS analysis wherein no Ag peak (367 eV) was observed from the H-SiNWs substrate (see Figure S5). The diameter of the SiNWs in the arrays is in the range 100−250 nm, while the wire length is around 25 μm. The morphology of the SiNW arrays is shown in Figure S2.

R6G as a typical SERS probe molecule has LUMO and HOMO levels of −3.40 and −5.70 eV, respectively.[13] These energy levels are consonant with the CB and VB of the SiNWs. Thus, CT between the SiNWs and R6G molecules is thermodynamically feasible at an excitation of 532 nm. In order to increase the efficiency of CT, SiNWs were further treated with hydrofluoric acid (HF) to fabricate H-SiNW arrays yielding a substrate on which the H atoms are electron-deficient and may serve as an electron sink.[23,27] Such a configuration would assist the separation of the photoinduced electrons and holes as well as improve electron tunneling, and further result in efficient CT. On the basis of such consideration, R6G was decorated onto the surface of H-SiNWs by immersing the H-SiNWs substrate into R6G solutions with variable concentrations at room temperature for 5 h. After rinsing off the excess R6G from the substrate with deionized water, the SERS experiment on R6G-decorated H-SiNWs substrate was immediately performed using a Renishaw Raman system-inVia-Reflex with excitation laser wavelengths of 532, 633, or 785 nm. The excitation intensities used were 0.125 mW at 532 nm, 0.325 mW at 633 nm, and 0.475 mW at 785 nm. The laser beam was focused to a spot about 3 μm in diameter with a 50× microscope objective. The Raman band of silicon wafer at 520 cm^{-1} was used to calibrate the spectrometer.

The results indicated that concentrations as low as 10^{-6} M R6G could be detected with excitation at 532 nm (see curve a in Figure 1a). Figure 1b clearly illustrates two thermodynamically allowed routes of the CT process between the R6G and H-SiNWs at the excitation wavelength. During the CT process from H-SiNWs to R6G, the electrons in the VB of the H-SiNWs were first stimulated by the incident light. Such stimulation results in the generation of electrons in the conduction band and holes in the valence band. The terminal hydrogen atoms of the H-SiNWs with a charge of −0.09 to −0.13 au may serve as an electron sink and assist the separation of photoinduced electrons and holes.[23] The excited electrons were quickly transferred from the H-SiNWs to the matching energy level of the LUMO of the R6G molecule through resonant tunneling. However, the electrons would eventually transit back to the H-SiNWs and recombine with the holes. During this process, a vibrational quantum of energy would transfer to the vibrational level of the R6G molecule, and a Raman photon would be radiated from the R6G molecule at some vibrationally state.[19] Similarly, during the CT process from the R6G to the H-SiNWs, the electrons occupying

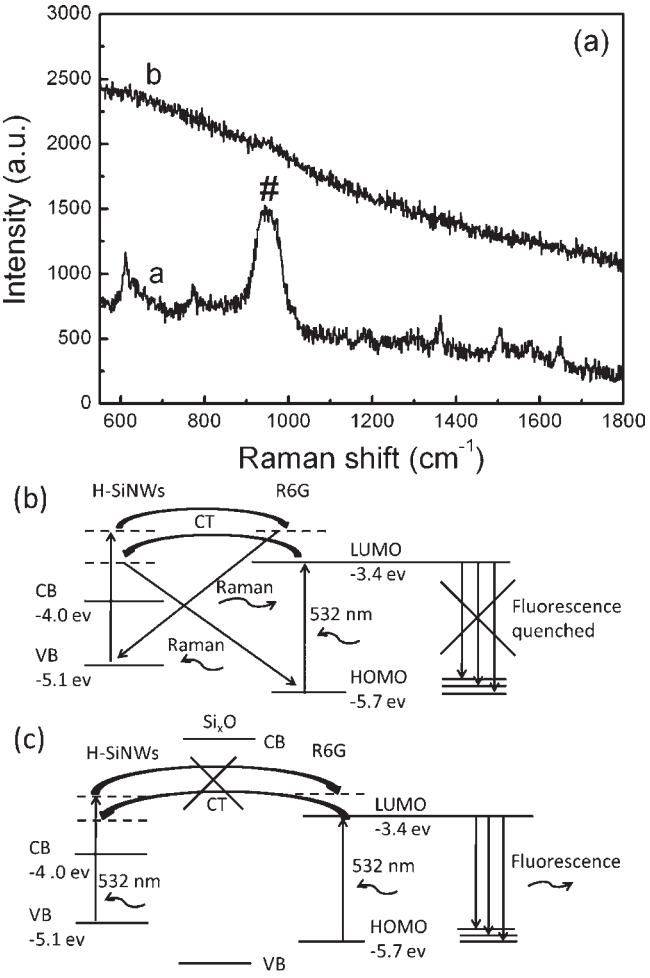

Figure 1. (a) Under the excitation of 532 nm, the SERS spectra of R6G with the concentration of 10^{-6} M obtained from the H-SiNWs substrate (curve a) and from the surface oxidized SiNWs substrate (curve b). Peak # belongs to the Si Raman peak. (b) Schematic illustration of the photoinduced CT process between R6G molecule and H-SiNWs with the excitation of 532 nm. (c) Schematic illustration of the oxide layer of Si inhibited the photoinduced CT process between R6G molecule and SiNWs.

the ground state of the R6G molecule are first excited from the HOMO to the LUMO by the incident light. Then, the excited electrons transfer quickly from the LUMO of the R6G molecule to the matching energy level above the CB of the H-SiNWs via resonant tunneling, which would be further accelerated by the attraction of the terminal hydrogen atoms of the H-SiNWs.[23] Subsequently, the electrons are transferred back to the vibrational energy level of the R6G molecule and radiated as a Raman photon with the R6G molecule at some vibrationally state. Both CTs from the R6G molecule to the SiNWs and from the SiNWs to the R6G molecule could contribute to the molecular polarizability tensor due to the vibronic coupling of the conduction band states $|S\rangle$ and valence band states $|S'\rangle$ with the molecular excited state $|K\rangle$ and molecular ground state $|I\rangle$ (details are provided in Supporting Information). When the frequency of the exciting light is higher than the molecular resonance ($\omega_0 > \omega_{IK}$), the polarizability tensor $\alpha_{\sigma\rho}$ can be written as $\alpha_{\sigma\rho} = A + B + C$, where A represents the contribution of the molecular resonance, and B and C represent the contributions from the photoinduced

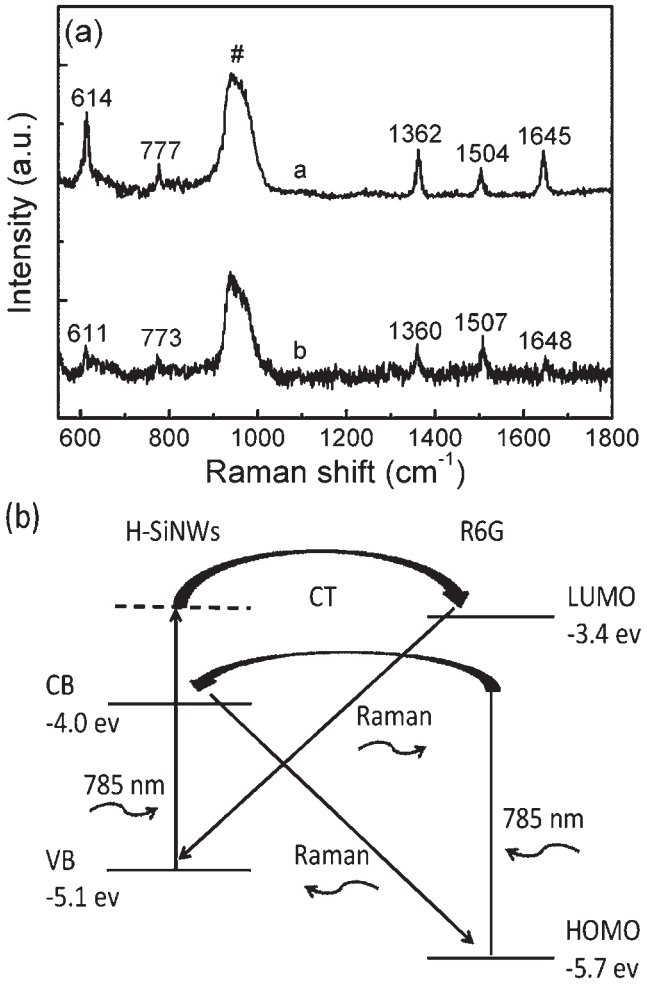

Figure 2. (a) Under the excitation of 785 nm, the SERS spectra of R6G with the concentration of 10^{-4} M obtained from the H-SiNWs substrate (curve a) and with the concentration of 10^{-3} M obtained from the surface oxidized SiNWs substrate (curve b). Peak # belongs to the Si Raman peak. (b) Schematic illustration of the photoinduced CT process from H-SiNWs to R6G with excitation of 785 nm.

CTs of the molecule-to-semiconductor and semiconductor-to-molecule, respectively (see Supporting Information eq 2). It is evident that the efficient transition of the excited electron between the R6G molecule and the SiNWs results in the occurrence of SERS.

It may be conjectured that the above transition would be prohibited if a barrier is inserted between the R6G and SiNWs, and as a result, no SERS would be detected. In order to verify this, an additional experiment was performed. The surface of the H-SiNWs substrate was oxidized before it was immersed into the R6G solution. On excitation with a 532 nm laser no Raman signal is observed; only the high intensity fluorescence of the R6G can be detected from the oxidized SiNWs substrate (see curve b in Figure 1a). Since the CB of the silicon oxide is higher than both the LUMO of the R6G and the CB of the SiNWs,[24] the CT process between the R6G and the SiNWs is prohibited by the oxide layer of Si (Figure 1c). Thus, no SERS was detected from such a sample configuration. This result further supports the idea that the CT processes play a critical role in SERS. Comparing the strong fluorescence from the oxidized SiNWs substrate and the lower baseline from the H-SiNWs substrate suggests that the fluorescence of the R6G attached to H-SiNWs is significantly quenched. Quenching of background fluorescence would enhance the ratio of the signal-to-noise and make it more sensitive to detect SERS of R6G on H-SiNWs substrates.

In order to further verify the above model of SERS from semiconductor nanostructures, dye N719 with a LUMO and HOMO of −3.85 eV and −5.40 eV, respectively,[28] was also utilized as a probing molecule to investigate the SERS from the H-SiNWs substrate. On the basis of the above discussion, the CTs from the N719 to the H-SiNWs substrate and the reverse, from the H-SiNWs substrate to the N719, are thermodynamically allowed, and the CT efficiency should also be enhanced by the abundance of terminal hydrogen atoms. The observation of SERS and H-SiNWs-induced fluorescence quenching of N719 (10^{-5} M) from the H-SiNWs substrate were also observed with excitation of 532 nm. Similarly, there was no SERS signal (except for the overwhelming fluorescence background of the N719) detected from the oxidized surface of SiNWs (see Supporting Information Figure S3).

Apart from the CT process, the molecular resonance Raman enhancement (RRS) is also involved in SERS, since R6G and N719 have strong absorptions at 532 nm, which would produce a large intramolecular resonance effect.[29−31] Such RRS may be avoided in the presence of CT by changing the excitation wavelength. For verification, the SERS of the R6G from H-SiNWs substrate was performed with excitation of 785 nm where the R6G has very little absorption.[13] Clear SERS of R6G at a concentration of 10^{-4} M can be observed from the H-SiNWs substrate (see curve a in Figure 2a). In order to evaluate the enhancement factor (EF) increased by CT, the H-SiNWs substrate was replaced by the SiNWs with an oxidized surface substrate in the above experiment and only a detection limit of 10^{-3} M can be achieved (see curve b in Figure 2a). Since the specific surface area of the surface oxidized SiNWs substrate is as large as that of the H-SiNWs substrate, and the R6G molecules were physically adsorbed on the surface of both substrates, a rough first-order enhancement factor (EF) of every peak can be approximately calculated using an improvement over the standard equation[32]

$$EF_{CT} = I_{H\text{-}SiNWs} C_{SixO} / I_{SixO} C_{H\text{-}SiNWs} \quad (1)$$

where $I_{H\text{-}SiNWs}$ and I_{SixO} are the Raman intensities of the specific band of the analyte adsorbed on the H-SiNWs substrates with and without surface oxidation, respectively. $C_{H\text{-}SiNWs}$ and C_{SixO} are, respectively, the concentrations of the R6G solution using substrates immersed for the same duration. On the basis of the above computation, EFs are in the range 8−28; for example, EF (611 cm^{-1}) = 28, EF (773 cm^{-1}) = 14, EF (1360 cm^{-1}) = 12, EF (1507 cm^{-1}) = 8, EF (1648 cm^{-1}) = 16. The line at 611 cm^{-1} represents an out-of-plane deformation vibration of the xanthene ring; the line at 773 cm^{-1} represents the out-of-plane C−H bend vibration, and the other three lines at 1507, 1360, and 1648 cm^{-1} represent the in-plane stretch vibrations of the xanthene ring, respectively.[29] Clearly, the enhancement of the two lines at 611 and 773 cm^{-1} from the R6G-decorated H-SiNWs substrate reveals a selective enhancement of different vibrational modes of the organic molecule during the CT enhancement process. It is known that the R6G molecule has a nearly planar xanthene ring to which most of the observed Raman vibrations can be assigned. Obviously, this part of the molecule lies flat on the surface of the substrate, and to some extent it could be considered as a plane of symmetry.[33] According to the symmetry point group C_s, the

in-plane vibrations are totally symmetric (a′) and the out-of-plane vibrations are not totally symmetric (a″).[33] Since the charge-transfer transition dipole is perpendicular to the molecular plane, the Herzberg−Teller selection rules predict that the a″ vibrations at 611 and 773 cm^{-1} will be more selectively enhanced, as observed.[33−35] As the contribution of the RRS is excluded from the SERS, the detection limitation on the H-SiNWs for R6G is worse. It is notable that the frequency of the exciting light is far from the molecular resonance ($\omega_0 < \omega_{IK}$) in this case. Nevertheless the CT process can still play a critical role in the Raman enhancement produced by the H-SiNWs as shown in Figure 2b. The electron sink effect of the terminal hydrogen atoms of the H-SiNWs assist the separation of the photoinduced electrons and holes as well as accelerate the electron tunneling, and further promote the CT process. As a result of vibronic coupling of the $|S\rangle$ and $|S'\rangle$ with the $|K\rangle$ and $|I\rangle$, the molecular excited state K can be considered to be a silicon conduction band state S. Concomitantly the molecular ground state I can be considered to be a silicon valence band state S'. Accordingly, the CTs from R6G molecules to the SiNWs substrate as well as the reverse (from the SiNWs substrate to R6G molecules) contribute to the molecular polarizability tensor. A similar molecular resonance contribution to the polarizability tensor can also be expected under these circumstances. The polarizability tensor $\alpha_{\sigma\rho}$ in this case can be expressed as $\alpha_{\sigma\rho} = A_m + A_s + B' + C'$, where A_m and A_s represent the similar molecular resonance contributions from the photoinduced CT of the molecule-to-semiconductor and the semiconductor-to-molecule, respectively, B' and C' represent the contributions from the photoinduced CTs of the molecule-to-semiconductor and the semiconductor-to-molecule, respectively (see Supporting Information eq 3). Moreover, it should be noted that the shift of the characteristic Raman peaks and the vibration dependence of the enhancement factors are convincing evidence for the CT process in the chemical enhancement mechanism.[13,36]

In order to further confirm the CT mechanism in SERS, SERS from H-SiNWs substrates under different excitations (532, 633, and 785 nm) were compared, and the results are shown in the Figure S4a. By changing the energy of excitation, the influence of the degree of matching between the incident photon and the band gap on the CT process can be determined. The results revealed that the SERS intensity decreased as the degree of matching is reduced (see Supporting Information Figure S4a). Moreover, from a comparison with the relatively weak intensities of the lines at 611 and 773 cm^{-1} in the Raman scattering spectrum of R6G powders (see Supporting Information Figure S4b), the enhancement of the two lines in SERS spectra demonstrated that a strong CT process has occurred.[33−35]

In the above SERS experiments, R6G and N719 were attached by physical adsorption on the H-SiNWs. It can be envisaged that even stronger SERS would be achieved if the probe molecules can be covalently bonded onto the surface of the H-SiNWs yielding a more efficient CT. Utilizing the available Si−H sites as chemical sites, an organic monolayer could be covalently bonded to the Si surface via a chemical method.[37] The 4-aminothiophenol (PATP) as a chemosorption probe molecule in SERS has a thiol group.[38] Such a functional group can be utilized to covalently bond the PATP to the Si substrate. With the charge on the H atom of the H-SiNWs in the range −0.09 to −0.13 au,[27] the abundant Si−H bonds on the surface of the SiNWs may provide points of attachment of PATP molecules by the Si−S linkages through a nucleophilic substitution reaction of the thiol group. This would be similar to the case with which alkanethiols

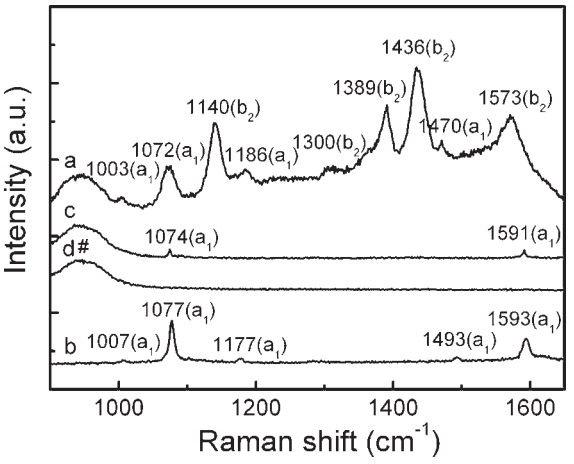

Figure 3. SERS spectra obtained from the PATP-chemisorbed H-SiNWs substrate (curve a). The characteristic Raman peaks of PATP powders (curve b). The SERS spectra obtained from the H-SiNWs substrate physically adsorbed with PATP (curve c). The SERS spectra obtained from the surface oxidized SiNWs with decorated PATP using the chemical reaction at 90 °C for 5 h (curve d). Peak # belongs to the Si Raman peak.

($CH_3(CH_2)_{n-1}SH$) can be covalently bonded to the HF-treated Ge surface to form a high-quality molecular monolayer by Ge−S bonds.[39] As the LUMO and HOMO of PATP molecule are at −3.03 and −7.16 eV, respectively,[36] under the excitation of 532 nm, the molecular resonance Raman enhancement could be ignored, and thus only the CT process from the SiNWs to the PATP molecules is thermodynamically allowed. In this case, the CT of the SiNWs-to-molecule could contribute to the molecular polarizability tensor due to the vibronic coupling of the $|S'\rangle$ with $|I\rangle$. The polarizability tensor $\alpha_{\sigma\rho}$ can be written as $\alpha_{\sigma\rho} = A_s + C'$ (see Supporting Information eq 3). In order to corroborate the above consideration, the H-SiNWs substrate was immersed into a PATP solution (10^{-3} M) for 5 h at 90 °C. After that, ultrasonic cleaning with solvent (acetonitrile) was employed to completely remove the unreacted molecules from the H-SiNWs substrate.[40] By this process, only the covalently bonded PATP molecules are left on the surface of the SiNWs; this was verified by the results of the angle-resolved XPS analysis (see Supporting Information Figure S5). The SERS from the PATP-chemisorbed H-SiNWs substrate was performed with excitation of 532 nm. The excitation intensity was 0.625 mW. The results show that in addition to the enhancement of the lines at 1003, 1072, 1186, and 1470 cm^{-1}, which are normally assigned as a_1 modes,[41−44] enhancements of the other five lines at 1573, 1436, 1389, 1300, and 1140 cm^{-1} are also observed (see curve a in Figure 3) compared to the Raman spectra from PATP powders (see the curve b in Figure 3). For comparison, the H-SiNWs substrate was immersed into the PATP solution (10^{-3} M) at room temperature for 5 h without the chemical reaction. In this way, the PATP molecules were simply physically adsorbed on the surface of the H-SiNWs. It was found that only weak a_1 modes located at 1074 and 1591 cm^{-1} could be observed (see curve c in Figure 3), and the other five lines observed from PATP-chemisorbed H-SiNWs substrate cannot be detected. Moreover, it was also found that no SERS could be detected at the above concentration after the oxide layer of the SiNWs was inserted between the PATP and the SiNWs (see the curve d in Figure 3). Obviously, the CT between the PATP and SiNWs was inhibited by the oxide layer, similar to the case discussed

dx.doi.org/10.1021/ja2057874 |J. Am. Chem. Soc. 2011, 133, 16518–16523

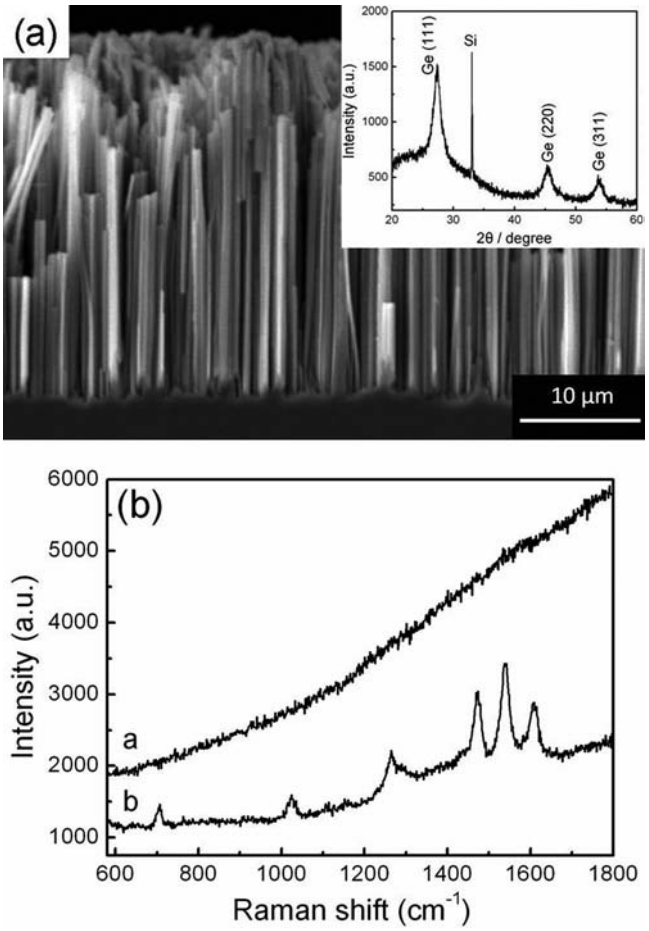

Figure 4. (a) SEM image of the side view of the GeNT arrays fabricated on the template of SiNWs with oxide layer. The inset is the X-ray diffraction pattern of the GeNT arrays. (b) The SERS spectra of N719 with the concentration of 10^{-5} M under the excitation of 532 nm obtained from the surface oxidized GeNT arrays as substrate (curve a), and from the H-GeNT arrays substrate (curve b).

above. Normally the five lines are attributed to all of the nontotally symmetric b_2 modes of the benzene ring vibrations of the PATP.[38−41] Although, recently there have been a series of studies on the SERS of PATP in which the PATP was believed to undergoes a photoinduced dimerization and p,p′-dimercaptoazobenzene (DMAB) was formed in the presence of Ag. The lines previously assigned as b_2 modes in PATP were reassigned as the symmetric modes (a_g) of the DMAB.[45−47] However, the fact that significant enhancement of b_2 modes can be observed only from PATP chemisorbed on H-SiNWs substrate and not with the PATP physically attached to substrates indicates that a strong CT process has taken place in our system based on the Herzberg−Teller selection rules.[20,44] Also, these vibrations are indeed attributed to the b_2 mode of the PATP, which is similar to the observation of the metal-PATP system investigated by density functional theory (DFT).[36] In addition, the more remarkable relative shifts of Raman peaks (such as the 1072 cm^{-1} peak of curve a in Figure 3) from the PATP-chemisorbed SiNWs substrate also demonstrate that the CT process using chemical modification is stronger than that merely using physical absorption.

SERS from both n-type and p-type H-SiNWs has been investigated in our experiments. The results indicated that both n-type and p-type H-SiNWs could give rise to SERS, and the difference is not obvious. For example, in the H-SiNWs-R6G system, SERS from the p-type H-SiNWs is as strong as the SERS from n-type H-SiNWs. This observation could be rationalized as follows: In the n-type H-SiNWs-R6G system, the CT from the n-type H-SiNWs to the R6G molecule would dominate the CT process. However in the p-type H-SiNWs-R6G system, the CT from the R6G molecule to H-SiNWs would dominate the CT process. Thus, p-type or n-type will not induce an obvious difference in the CT efficiency in the H-SiNWs−molecule system.

SiNWs can have a strong SERS by realizing the CT between the SiNWs and probe molecules; it was found that a strong SERS can also be observed from Ge nanostructures such as Ge nanotube (GeNT) arrays. The GeNT arrays used here were fabricated by thermally evaporating Ge on the template of the SiNWs with an oxide layer. The morphologies of the GeNT arrays are shown in Figure 4a. The X-ray diffraction shows that the GeNT arrays have a cubic crystal structure with lattice constant of a = 0.565 nm (inset of Figure 4a). In order to achieve efficient CT, the GeNT arrays are treated by HF to form H-terminated GeNT (H-GeNT) arrays. The dye N719 was utilized as the probe molecule to investigate the SERS from such a substrate. It is known that the VB and the CB of the GeNT arrays are −4.5 and −3.84 eV, respectively.[24] The CT process between N719 molecules and H-GeNT arrays should be thermodynamically allowed at an excitation of 532 nm, similar to the CT process between the H-SiNWs and R6G molecules. N719 molecules were adsorbed on the surface of the H-GeNT arrays by immersing the H-GeNT arrays substrate into a 10^{-5} M solution of N719 at room temperature for 5 h. Results (Figure 4b) showed that a remarkable SERS from the H-GeNT arrays substrate was achieved. For comparison, SERS cannot be observed from the oxidized surface of a GeNT arrays substrate. Just as in the case discussed above, the CT between the N719 and GeNT arrays was obviously inhibited by the oxide layer. This enhancement from the H-GeNT arrays demonstrated that efficient CT between the N719 probe molecules and the Ge nanostructured substrate can be realized. A similar experiment using R6G as a probe molecule to investigate the SERS of H-GeNT arrays was also carried out with excitation of 532 nm. The obvious SERS and the H-GeNT arrays-induced fluorescence quenching of R6G (10^{-6} M) are also detected. No SERS signal except the overwhelming fluorescence background of R6G can be observed from the oxidized GeNT arrays (see Supporting Information Figure S6). The presence of SERS from the H-GeNT arrays substrate further corroborates the molecule−semiconductor model discussed above, and suggests that decorating the hydrogen atoms on the surface of the GeNT arrays is an effective approach to increase SERS from nanostructured semiconducting substrates.

It is worthwhile to point out that the nanostructured Si and Ge provided a huge surface area on which abundant probe molecules can be attached by physical or chemical means. For physical adsorption, the numerous terminal hydrogen atoms on the surface of the H-SiNW and H-GeNT arrays may serve as an electron sink to assist the separation of photoinduced electrons and holes and promote the CT from the substrate to the adsorbed molecules. Alternatively, these surfaces can accelerate the electron tunneling and improve the CT from the adsorbed molecules to the substrate. For chemical adsorption, the numerous terminal hydrogen atoms may serve as chemical bonding sites to provide covalent attachment of target molecules on the nanostructures. This is the reason that only H-SiNW and H-GeNT arrays but not Si and Ge wafers can significantly enhance the Raman signal.

CONCLUSIONS

Our model of SERS in molecule−semiconductor systems allows the contribution of the CT process to the molecular polarizability tensor to be calculated, and demonstrates the possibility of utilizing Si and Ge substrates to cause SERS to arise. It was found that, by exploiting terminal hydrogen atoms on the surface of H-SiNW and H-GeNT arrays, an efficient CT process between the molecules and the nanostructured Si or Ge substrates can be successfully realized, and SERS from such substrates can be detected. The appearance and obvious enhancement of the b_2 modes of the PATP molecules covalently bonded to the H-SiNWs substrate indicates that the CT efficiency and the SERS intensities could be improved significantly when molecules are chemically bonded to the surface of the nanostructured semiconductor substrate. It is believed that transitioning appropriate SERS substrates from the noble metals to Si and Ge semiconductors will extend SERS to promising applications in the realm of biomedical detection.

ASSOCIATED CONTENT

Supporting Information. Model and the calculation of SERS in the semiconductor−molecule system; the SEM image of the SiNW arrays; the SERS spectra of N719 obtained from the H-SiNWs substrate; the SERS spectrum of R6G from the H-SiNWs substrate with different excitation lines; the angle-resolved XPS analysis of the H-SiNWs substrate before and after chemisorbing PATP; the SERS spectra of R6G obtained from the H-GeNT arrays substrate.This material is available free of charge via the Internet at http://pubs.acs.org.

AUTHOR INFORMATION

Corresponding Author
shiws@mail.ipc.ac.cn

ACKNOWLEDGMENT

This work was supported by Chinese Academy of Sciences, NSFC (Grants 10874189, 50902134, 61025003, and 21103211), National Basic Research Program of China (973 Program) (Grants 2010CB934103 and 2012CB932400), and Beijing Natural Science Foundation (Grant 2102043).

REFERENCES

(1) Nie, S.; Emory, S. R. *Science* **1997**, *275*, 1102.
(2) Michaelsk, A. M.; Nirmal, M.; Brus, L. E. *J. Am. Chem. Soc.* **1999**, *121*, 9932.
(3) Fleishchmann, M.; Hendra, P. J.; McQuillan, A. J. *Chem. Phys. Lett.* **1974**, *26*, 163.
(4) Wenning, U.; Pettinger, B.; Wetzel, H. *Chem. Phys. Lett.* **1980**, *85*, 473.
(5) Ren, B.; Lin, X. F.; Yang, Z. L.; Liu, G. K.; Aroca, R .F.; Mao, B. W.; Tian, Z. Q. *J. Am. Chem. Soc.* **2003**, *125*, 9598.
(6) Haynes, C. L.; Van Duyne, R. P. *Nano Lett.* **2003**, *3*, 939.
(7) Quagliano, L. G. *J. Am. Chem. Soc.* **2004**, *126*, 7393.
(8) Wang, Y. F.; Ruan, W. D.; Zhang, J. H.; Yang, B.; X, W. Q.; Zhao, B.; Lombardi, J. R. *J. Raman. Spectrosc.* **2009**, *40*, 1072.
(9) Musumeci, A.; Gosztola, D.; Schiller, T.; Dimitrijevic, N. M.; Mujica, V.; Martin, D.; Rajh, T. *J. Am. Chem. Soc.* **2009**, *113*, 6040.
(10) Fu, X. Q.; Bei, F. L.; Wang, X.; Yang, X. J.; Lu, L. *J. Raman. Spectrosc.* **2009**, *40*, 1290.
(11) Fang, J. Y.; Chu, P. K. *Small* **2010**, *6*, 2080.
(12) Alvarez, S. D.; Derfus, A. M.; Schwartz, M. P.; Bhatia, S. N.; Sailor, M. J. *Biomaterials* **2009**, *30*, 26.
(13) Ling, X.; Xie, L. M.; Fang, Y.; Xu, H.; Zhang, H. L.; Kong, J.; Dresselhaus, M. S.; Zhang, J.; Liu, Z. F. *Nano Lett.* **2010**, *10*, 553.
(14) Campion, A.; Kambhampati., P. *Chem. Soc. Rev.* **1998**, *27*, 241.
(15) Moskovits, M. *Rev. Mod. Phys.* **1985**, *57*, 783.
(16) Braun, G.; Pavel, I.; Morrill, A. R.; Seferos, D. S.; Bazan, G. C.; Reich, N. O.; Moskovits, M. *J. Am. Chem. Soc.* **2007**, *129*, 7760.
(17) Svedberg, F.; Li, Z. P.; Xu, H. X.; Käll, M. *Nano Lett.* **2006**, *6*, 2639.
(18) Musumeci, A.; Gosztola, D.; Schiller, T.; Dimitrijevic, N. M.; Mujica, V.; Martin, D.; Rajh, T. *J. Am. Chem. Soc.* **2009**, *131*, 6040.
(19) Persson, B. N. J.; Zhao, K.; Zhang, Z. Y. *Phys. Rev. Lett.* **2006**, *96*, 207401.
(20) Lombardi, J. R.; Birke, R. L.; Lu, T.; Xu, J. *J. Chem. Phys.* **1986**, *84*, 4174.
(21) Lombardi, J. R; Birke, R. L. *J. Chem. Phys.* **2008**, *112*, 5605.
(22) Albrecht, A. C. *J. Chem. Phys.* **1961**, *34*, 1476.
(23) Shao, M. W.; Cheng, L.; Zhang, X. H.; Ma, D. D. D.; Lee, S. T. *J. Am. Chem. Soc.* **2009**, *131*, 17738.
(24) Van de Walle, C. G. *Phys. Rev. B.* **1989**, *39*, 1871.
(25) Peng, K. Q.; Lu, A. J.; Zhang, R. Q.; Lee, S. T. *Adv. Funct. Mater.* **2008**, *18*, 3026.
(26) Geyer, N.; Huang, Z. P.; Fuhrmann, B.; Grimm, S.; Reiche, M.; Nguyen-Duc, T. K.; Johannes de Boor, J .; Leipner, H. S.; Werner, P.; Gosele, U. *Nano Lett.* **2009**, *9*, 3106.
(27) Zhang, R. Q.; Lu, W. C.; Zhao, Y. L.; Lee., S. T. *J. Phys. Chem. B* **2004**, *108*, 1967.
(28) Lenzmann, F.; Krueger, J.; Burnside, S.; Brooks, K.; Grätzel, M.; Gal, D.; Rühle, S.; Cahen, D. *J. Phys. Chem. B* **2001**, *105*, 6347.
(29) Jensen, L.; Schatz, G. C. *J. Phys. Chem. A* **2006**, *110*, 5973.
(30) Burns, A. R.; Jennison, D. R.; Stechel, E. B.; Li, Y. S. *Phys. Rev. Lett.* **1994**, *72*, 3895.
(31) Leon, C. P.; Kador, L.; Peng, B.; Thelakkat, M. *J. Phys. Chem. B* **2006**, *110*, 8723.
(32) Tian, Z. Q.; Gao, J. S.; Li, X. Q.; Ren, B.; Huang, Q. J.; Cai, W. B.; Liu, F. M.; Mao, B. W. *J. Raman Spectrosc.* **1998**, *29*, 703.
(33) Canamares, M. V.; Chenal, C.; Birke, R. L.; Lombardi, J. R. *J. Phys. Chem. C* **2008**, *112*, 20295.
(34) Weiss, A; Haran, G. *J. Phys. Chem. B* **2006**, *105*, 12348.
(35) Liang, E. J.; Ye, X. L.; Kiefer, W. *J. Phys. Chem. A* **1997**, *101*, 7330.
(36) Sun, Z. H.; Wang, C. X.; Yang, J. X.; Zhao, B.; Lombardi, J. R. *J. Phys. Chem. C* **2008**, *112*, 6093.
(37) Li, K. J.; Li, S. G.; Li, N.; Dixon, D. A.; Klein, T. M. *J. Phys. Chem. C* **2010**, *114*, 14061.
(38) Larsen, A. G.; Holm, A. H.; Roberson, M.; Daasbjerg, K. *J. Am. Chem. Soc.* **2001**, *123*, 1723.
(39) Han, S. M.; W. Ashurst, W. R.; Carraro, C.; Maboudian, R. *J. Am. Chem. Soc.* **2001**, *123*, 2422.
(40) Mu, L. X.; Shi, W. S.; Chang, J. C.; Lee, S. T. *Nano Lett.* **2008**, *8*, 104.
(41) Kim, K.; Lee, H. B.; Yoon, J. K.; Shin, D.; Shin, K. S. *J. Phys. Chem. C* **2010**, *114*, 13589.
(42) Yoon, J. K.; Kim, K.; Shin, K. S. *J. Phys. Chem. C* **2009**, *113*, 1769.
(43) Kim, K.; Yoon, J. K.; Lee, H. B.; Shin, D.; Shin, K. S. *Langmuir* **2011**, *27*, 4526.
(44) Osawa, M.; Matsuda, N.; Yoshii, K.; Uchida, I. *J. Phys. Chem. C* **1994**, *98*, 12702.
(45) Wu, D. Y.; Liu, X. M.; Huang, Y. F.; Ren, B.; Xu, X.; Tian, Z. Q. *Phys. Chem. C* **2009**, *113*, 18212.
(46) Fang, Y.; Li, Y.; Xu, H.; Sun, M. *Langmuir* **2010**, *26*, 7737.
(47) Huang, Y. F.; Zhu, H. P.; Liu, G. K.; Wu, D. Y.; Ren, B.; Tian, Z. Q. *J. Am. Chem. Soc.* **2010**, *132*, 9244.